

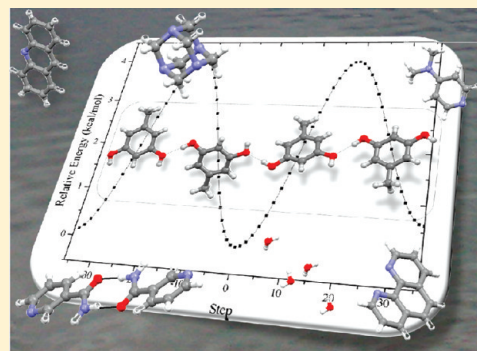
Polymorphs, Pseudopolymorphs, and Co-Crystals of Orcinol: Exploring the Structural Landscape with High Throughput Crystallography

Arijit Mukherjee, Paweł Grobelny, Tejender S. Thakur, and Gautam R. Desiraju*

Solid State and Structural Chemistry Unit, Indian Institute of Science, Bangalore 560 012, India

Supporting Information

ABSTRACT: An extensive search of the structural landscape of orcinol, 5-methyl-1,3-dihydroxybenzene, has been carried out with high throughput techniques. Polymorphs, pseudopolymorphs (solvates), and co-crystals are described. Several packing modes driven by O—H \cdots N hydrogen bonds were identified for the orcinol–N-base co-crystals and their hydrates. In these several structural variations, the OH group conformations in the orcinol molecule were found to depend on the choice of co-formers and the crystallization conditions employed. The structural landscape of a molecule is properly described by a sufficiently large number of related crystal structures, and high throughput crystallization followed by rapid structure determinations enables one to access these structures efficiently. Any understanding of this landscape would enable the crystal engineer to reasonably anticipate crystal structures of benzene-1,3-diol co-crystals with N-bases.



■ INTRODUCTION

For any given single component or multicomponent chemical entity, there are many ways in which three-dimensional (3-D) crystal packing may possibly be achieved. Each unique crystal structure represents a stationary point on the crystal energy landscape¹ along which one may move during the process of crystallization or in a phase transformation. The main aim of this study is to obtain some degree of control over the structural variables of a representative system. A sufficiently large collection of data points improves and strengthens our understanding of the landscape. It is not easy to explore all putative packing arrangements within a finite time frame and as remarked pithily by McCrone, “the number of polymorphic forms known for a given compound is proportional to the time and money spent in research on that compound”.² One might just as well replace the words “polymorphic forms” with the words “pseudopolymorphs” or “co-crystals”. High throughput crystallography provides an economical way to explore the landscape.³ Additionally, computed crystal structures for a given system can provide a foreground for planning experimental studies; such forms are generated in crystal structure prediction (CSP) exercises.⁴ The present study discusses polymorphs, pseudopolymorphs, and co-crystals of orcinol (5-methyl-1,3-dihydroxybenzene, 5-methylresorcinol). This naturally occurring phenolic compound is found in many species of lichen. Orcinol derivatives are used as external antiseptics for skin diseases. 4-Hexyl-1,3-dihydroxybenzene (*n*-hexylresorcinol) is a constituent of some throat lozenges. Orcinol is used widely in the production of the dye orcein and as a reagent in Bial’s test for pentoses and urinoids.

Phenols are capable of forming O—H \cdots Y (Y = O, N, S, halogen) hydrogen bonds. Among these, the O—H \cdots N hydrogen bond is one of the most robust and well-studied synthons in crystal engineering.^{5,6} An additional feature of interest in orcinol is the rotational flexibility of the hydroxy groups that leads to conformational isomers (*syn* or *anti*), so that there are three conformers A, B, and C possible for the molecule (Scheme 1).

■ EXPERIMENTAL DETAILS

Materials. Orcinol monohydrate (97%) was purchased from Lancaster, (U.K.) and used as such in all crystallization experiments. All other reagents were obtained from commercial suppliers and used without further purification.

Crystallization. The anhydrous form I of orcinol was obtained by dissolving the compound in a minimum amount of CHCl₃ followed by slow evaporation at room temperature. Orcinol form II crystals were obtained by slow evaporation from a nitromethane solution kept at \sim 5 °C. Crystals of orcinol monohydrate were grown from MeOH (LR grade) at room temperature.

High throughput techniques (high throughput crystallization and high throughput crystal structure analysis) were employed to sample the structural landscape of orcinol conformations especially with regard to co-crystallization with N-bases. A large number of N-bases were selected. In each case crystallization was attempted under various experimental conditions. For each batch, several samples were taken on the

Received: March 22, 2011

Revised: April 12, 2011

Published: April 13, 2011

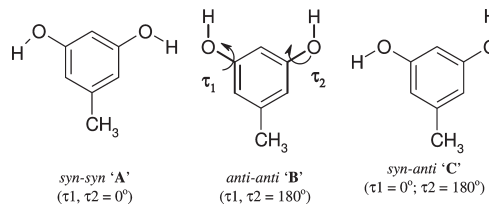
diffractometer. As soon as a new unit cell was obtained, full data were collected. In this way, a large number of new crystals including polymorphs were identified. Solvates were also obtained in many cases. Contrary to several recent reports, we never obtained a new polymorph of a pure substance during a co-crystallization attempt.

Co-crystallization experiments of orcinol with various co-formers were performed with 1:1, 2:1, and 1:2 molar ratios in various common organic solvents. The details of the co-crystallization experiments are given in the Supporting Information. Various crystallization techniques such as solution crystallization, neat grinding, solvent drop-grinding, and vapor diffusion methods were employed in order to obtain good quality single crystals for the X-ray diffraction studies (see Table 1).

Single Crystal X-ray Diffraction. Single crystal data for crystals were collected on a Rigaku Mercury375R/M CCD (XtaLAB mini) diffractometer using graphite monochromated Mo-K α radiation, equipped with a Rigaku low temperature gas spray cooler. In these cases, data were processed with the Rigaku CrystalClear software.⁷ Structure solution and refinements were performed using SHELX97⁸ using the WinGX suite.⁹ The ORTEPs and the additional experimental details are provided in the Supporting Information (Figure S1 and Table S2).

Computational Details. Geometry optimizations were performed without any symmetry constraints at the B3LYP/6-311++(2df,2pd)¹⁰

Scheme 1. Three Possible Conformations of Orcinol



basis set using the Gaussian 09 package.¹¹ Optimizations were performed using direct inversion of iterative subspace (GDIIS) method¹² with convergence criteria (threshold values: maximum force = 0.000015 a.u.; rms force = 0.00001 a.u.; maximum displacement = 0.00006 a.u.; rms displacement = 0.00004 a.u.). The relaxed linear potential energy surface scans for OH group rotation were performed at the same level of theory.

RESULTS

Orcinol exists in three conformations *syn-syn*, *anti-anti*, and *syn-anti* (**A–C**; Scheme 1). Computation done at the B3LYP/6-311++(2df,2pd) level shows that *syn-anti* conformer (**C**) is the

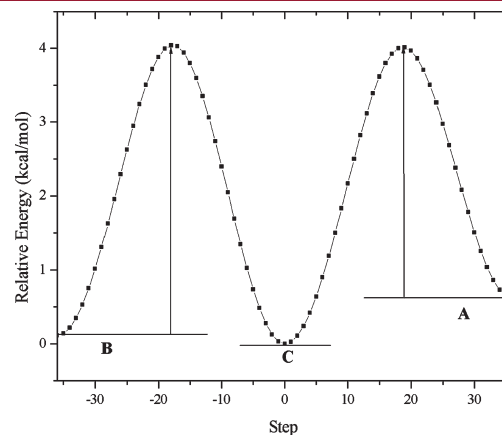
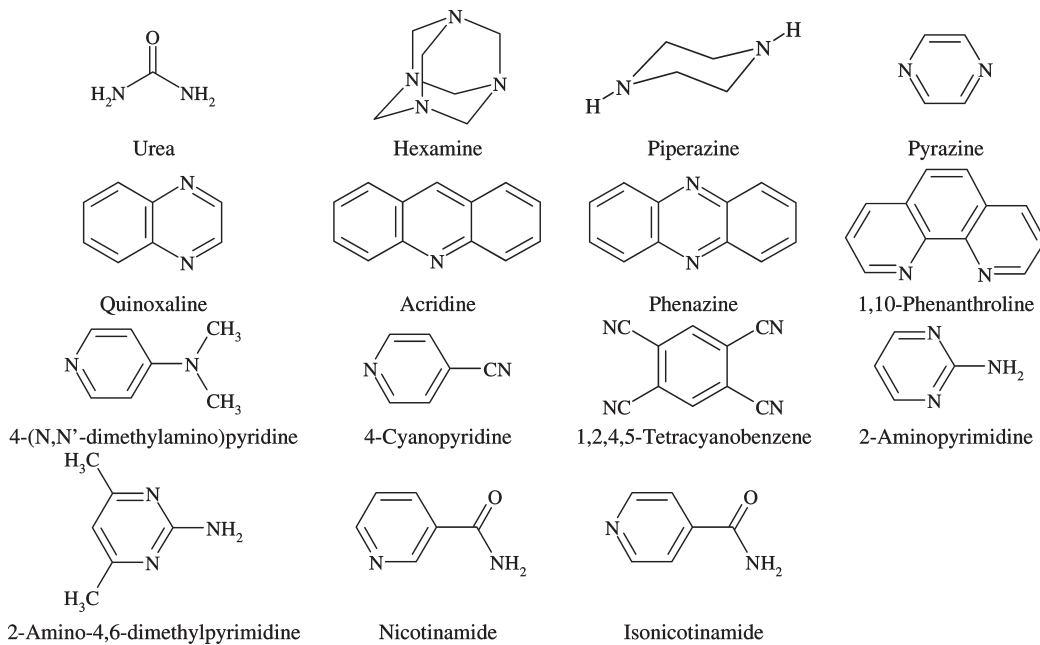


Figure 1. Relaxed linear potential energy scan for OH group rotation calculated at the B3LYP/6-311++G(3df,2pd) level of theory between conformations **A**, **B**, and **C** of orcinol.

Table 1. Crystal Structure Details for the Polymorphs, Pseudopolymorphs, and Co-Crystals of Orcinol

structure	space group	<i>a</i> (Å)	<i>b</i> (Å)	<i>c</i> (Å)	α (deg)	β (deg)	γ (deg)	<i>V</i> (Å ³)	<i>R</i>
1a	$I\bar{4}$	20.060(3)	20.060(3)	6.423(1)	90	90	90	2584.6(8)	0.06
1b	$P2_12_12_1$	13.78(1)	16.17(2)	24.55(2)	90	90	90	5473(9)	0.09
1c	$P2_1/c$	9.899(2)	7.951(2)	9.171(2)	90	96.88(3)	90	716.6(3)	0.04
2	$C2/c$	16.602(3)	10.546(2)	7.070(1)	90	99.30(3)	90	1221.6(4)	0.09
3	$P2_1/n$	7.200(1)	7.599(2)	35.894(7)	90	91.01(3)	90	1963.5(7)	0.06
4	$P2_1/c$	7.495(2)	17.596(5)	14.389(4)	90	97.656(7)	90	1880.7(9)	0.05
5	$Pccn$	17.572(3)	21.702(4)	7.065(1)	90	90	90	2694.2(9)	0.04
6	$P\bar{1}$	8.7636(7)	10.9081(9)	13.317(1)	112.508(8)	104.169(7)	92.570(7)	1126.6(2)	0.05
7	$P\bar{1}$	8.4494(9)	12.362(1)	19.748(2)	83.323(7)	77.689(7)	89.497(6)	2001.3(4)	0.06
8a	$P2_1/c$	10.498(8)	8.887(7)	15.557(9)	90	113.80(4)	90	1328(2)	0.05
8b	$C2/c$	17.213(3)	8.478(2)	21.650(4)	90	91.04(3)	90	3159(1)	0.07
8c	$C2/c$	13.845(3)	9.612(2)	15.059(3)	90	97.096(7)	90	1988.6(7)	0.04
8d	$P\bar{1}$	7.859(2)	8.146(2)	16.239(4)	83.929(6)	81.521(6)	86.524(6)	1021.3(4)	0.11
9a	$P\bar{1}$	7.837(2)	9.702(3)	17.830(5)	98.229(7)	100.908(7)	103.819(7)	1267.2(6)	0.11
9b	Pna_2_1	9.3390(7)	25.441(2)	13.750(1)	90	90	90	3267.0(4)	0.04
10a	$P\bar{1}$	8.282(1)	10.909(1)	16.600(2)	99.961(9)	96.163(7)	93.253(5)	1464.3(3)	0.05
10b	$P\bar{1}$	7.926(2)	12.560(3)	16.750(3)	96.16(3)	99.97(3)	98.56(3)	1608.8(6)	0.13
11	$C2/c$	33.630(7)	7.260(2)	15.358(3)	90	95.65(3)	90	3732(1)	0.06
12	$C2/c$	7.246(1)	12.316(2)	12.590(2)	90	96.268(7)	90	1116.8(3)	0.04
13	$P2_1/n$	6.997(1)	8.580(2)	13.531(3)	90	95.16(3)	90	809.0(3)	0.04
14a	$P2_1/c$	7.070(1)	14.274(3)	19.730(4)	90	99.05(3)	90	1966.4(7)	0.07
14b	$P\bar{1}$	8.2900(17)	9.990(2)	12.690(3)	104.66(3)	103.82(3)	96.33(3)	970.9(4)	0.11
15	$P\bar{1}$	8.176(2)	9.294(2)	16.888(3)	102.32(3)	102.03(3)	93.53(3)	1218.6(5)	0.08
16	$P2_1/c$	13.783(7)	13.520(7)	15.981(6)	90	124.11(3)	90	2466(2)	0.05

Scheme 2. Chemical Structures of Co-formers Used in This Study



most stable. The relative stabilities of the three conformers **A**, **B**, and **C** are 0.6, 0.1, and 0.0 kcal/mol, respectively. An estimate of the interconversion barrier in the gas phase was obtained from the relaxed linear potential energy scan done for the dihedrals (τ_1 and τ_2 , Scheme 1) from 0 to 180° with a step size of 5° performed at the same level of theory (Figure 1). Calculation shows a barrier of 4.03 and 4.01 kcal/mol for the interconversion from conformer **C** to **A** and from conformer **C** to **B**, respectively. The low energy rotational barrier hints at the nearly equal probabilities for the existence of conformations **A** and **B** under normal conditions. Hence, any preference for a particular conformation or mixture of conformations could possibly be assumed from the solvent or co-former driven conformation selection. The orcinol molecule will selectively adopt any of these three conformations as per the requirement of the growing nuclei such that the intermolecular interactions are well optimized to suit the supramolecular environment. This can lead to numerous packing possibilities during the crystallization event. Exploring each of these possibilities for a particular orcinol co-former system is a difficult task. However, some information about these motifs can be indirectly sampled by performing co-crystallization experiments with a large number of similar co-formers. One attempts to perturb the system chemically in order that the structural landscape is more easily accessed.

For a better understanding of the landscape, we tried both crystallization and co-crystallization experiments under various conditions. Compounds chosen for co-crystallization are shown in Scheme 2. Lattice parameters for the crystal structures are given in Table 1. The choice of N-base co-formers was restricted only to rigid molecules in the present study as the inclusion of co-former flexibility may further complicate the situation and lead to loss of generality. Information about the data collection and structure refinements are provided in the Supporting Information, Table S2.

Orcinol Form I (1a). Crystals of the anhydrous form I were grown from CHCl_3 solution. Form I crystallizes in the tetragonal space group, $I\bar{4}$ with $Z' = 2$. Both symmetry independent

molecules adopt the *syn-anti* conformation. As expected, the crystal structure is dominated by $\text{O}-\text{H}\cdots\text{O}$ hydrogen bonds (Figure 2). The symmetry independent molecules are linked along 2_1 by two sets of nearly equal $\text{O}-\text{H}\cdots\text{O}$ hydrogen bonds (Table 2).

Orcinol Form II (1b). A second form of anhydrous orcinol with $Z' = 8$ in space group $P2_{1}2_{1}2_{1}$ was obtained from nitromethane. This is not the first instance in our experience when nitromethane provides an entirely different polymorphic structure.¹³ Of the eight symmetry independent molecules, four adopt the stable *syn-anti* conformation and there are two molecules each with *syn-syn* and *anti-anti* conformations. This structure is characterized by a one-dimensional (1-D) chain of $\text{O}-\text{H}\cdots\text{O}$ hydrogen bonds consisting of a sequence of four symmetry independent molecules in the order *syn-syn*, *anti-anti*, *syn-anti* and *syn-anti* (Figure 2c). These chains extend in the other two dimensions and are cross-linked to form a 3-D network (Figure 2d). Form II has several $\text{O}-\text{H}\cdots\text{O}$ interactions of varying strengths ranging from a very short and linear $\text{O}-\text{H}\cdots\text{O}$ bond (1.69 \AA , 2.675 \AA , 175°) to longer and bent $\text{O}-\text{H}\cdots\text{O}$ interactions (1.88 \AA , 2.746 \AA , 146°). Besides these stronger hydrogen bonds, there are weak $\text{C}-\text{H}\cdots\text{O}$ and $\text{C}-\text{H}\cdots\pi$ interactions (see Table 2). Form I (1a) can be considered to be the more stable form as indicated by its higher density ($\rho = 1.276 \text{ g/cm}^3$) and better packing (Kitaigorodskii packing index (KPI),¹⁴ 68%). For form II (1b), $\rho = 1.205 \text{ g/cm}^3$ and KPI = 64%. Lattice energy calculations performed on these structures also support the higher stability, -0.6 kcal/mol , for form I (1a); see Supporting Information.

Orcinol Monohydrate (1c). Most attempts to obtain anhydrous orcinol resulted in the formation of orcinol monohydrate, which crystallizes in the monoclinic space group $P2_1/c$. Like in form I, the molecules adopt a *syn-anti* conformation. In the hydrate, orcinol forms a 1-D tape of $\text{O}-\text{H}\cdots\text{O}$ hydrogen bonds consisting of a four-membered ring having a topology $R_4^4(12)$ and with intervening water molecules. These water molecules also act as linkers between adjacent layers and facilitate crystal

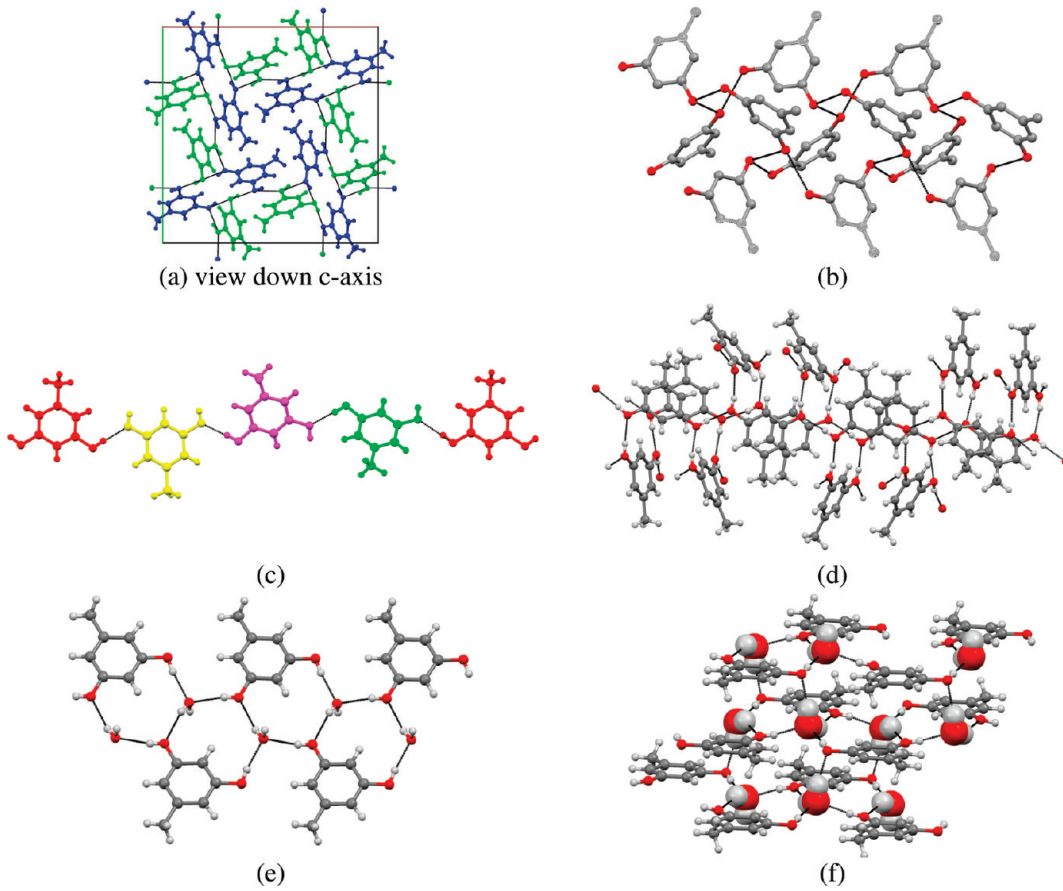


Figure 2. Crystal packing in orcinol (a–b) form I (1a); (c–d) form II (1b); and (e–f) orcinol monohydrate (1c). The symmetry independent molecules in orcinol forms I and II are color coded.

growth in the perpendicular direction (Figure 2). The penta-2,4-diyinyl 3,5-dihydroxybenzoate monohydrate (Cambridge Structural Database (CSD)¹⁵ refcode, ALOLUI) also forms similar a four-membered ring topology with water molecules acting as linkers between adjacent layers.

Orcinol–Urea 1:2 Co-Crystal (2). Orcinol–urea co-crystal is an excellent example of co-former driven conformation selection during crystallization. This co-crystal contains 0.5 molecules of orcinol (lying on a 2-fold axis) and one molecule of urea. The orcinol molecule adopts the least stable *syn-syn* conformation. The urea molecule retains the robust urea N–H \cdots O homodimer synthon observed in many urea co-crystals (Figure 3a). The hydrogen bond acceptor vacancies available in urea are fully satisfied in the tape motif. However, two of the N–H donor sites are left unoccupied within the motif. Thus, the only choice left for the orcinol molecule is to adopt the *syn-syn* conformation so as to incorporate itself between the urea dimer tapes. An alternative packing arrangement with an *anti-anti* or *syn-anti* conformation can also be envisaged but will require a heavy price to be paid in terms of energy, possibly with a high Z' structure and a disfavored packing resulting from the steric hindrance and long N–H \cdots O and O–H \cdots O interactions. The orcinol acts as a linker between parallel sets of urea dimer chains; this holds the structure with O–H \cdots O interactions trifurcated at the carbonyl oxygen acceptor of urea. The orcinol molecules are stacked in an antiparallel fashion with a short $\pi\cdots\pi$ interaction of 3.73 Å and a slippage of 1.24 Å.

The main purpose of the study was to explore possible pathways available during crystallization of orcinol with mono-N and bi-N-acceptor co-formers arising from the three conformations of orcinol. Using information obtained from the CSD on the resorcinol–urea co-crystal¹⁶ (CSD refcode BODSAO; obtained from acetone-methanol mixture) a deliberate co-crystallization attempt of orcinol with urea was performed (vapor diffusion method from methanol–hexane solvent) to direct the co-crystallization event to a predesigned crystal form with a more stable orcinol conformation. However, the orcinol–urea co-crystal shows striking dissimilarities with the known resorcinol–urea co-crystal. The orcinol molecule in orcinol–urea adopts the least stable *syn-syn* conformer A of very low probability in which the urea retains its robust N–H \cdots O dimer tape synthon. However, conformation C was observed for the resorcinol–urea co-crystal and the urea dimer tape is completely broken; the structure shows similarities to orcinol monohydrate (1c). The urea in the resorcinol–urea co-crystal behaves just like a water molecule forming a similar sheet topology and the free N–H group acts as linker between adjacent sheets.

Orcinol–1,2,4,5-Tetracyanobenzene 2:3 Co-Crystal (3). Orcinol forms a 2:3 co-crystal with 1,2,4,5-tetracyanobenzene in the space group P_{2_1}/n with 1.5 symmetry independent molecules of 1,2,4,5-tetracyanobenzene. Orcinol adopts the *syn-anti* conformation linking the two symmetry independent molecules of 1,2,4,5-tetracyanobenzene by O–H \cdots N hydrogen bonds and forming a tetrameric unit (Figure 3c). Out of the

Table 2. Intermolecular Interactions Found in the Crystal Structures (1–16) with Normalized H-Atom Positions

structure	interaction	H···A (Å)	X···A (Å)	X–H···A (deg)	symmetry code
1a	O1–H1o···O3	1.80	2.733(4)	157	$x, y, 1 + z$
	O2–H2o···O4	1.79	2.760(3)	171	$3/2 - x, 3/2 - y, -1/2 + z$
	O3–H3o···O2	1.82	2.770(3)	163	
	O4–H4o···O1	1.82	2.718(3)	151	$y, 1 - x, 2 - z$
1b	O1–H1o···O9	1.74	2.722(6)	173	
	O2–H2o···O4	1.88	2.746(5)	146	$3/2 - x, -y, 1/2 + z$
	O3–H3o···O14	1.84	2.767(5)	157	$2 - x, -1/2 + y, 3/2 - z$
	O4–H4o···O16	1.73	2.706(6)	171	$1/2 + x, 1/2 - y, 1 - z$
	O5–H5o···O7	1.74	2.718(6)	174	
	O6–H6o···O2	1.81	2.761(6)	163	$-1/2 + x, 1/2 - y, 2 - z$
	O7–H7o···O1	1.79	2.744(7)	163	$1 - x, 1/2 + y, 3/2 - z$
	O8–H8o···O13	1.76	2.727(5)	168	$3/2 - x, 1 - y, -1/2 + z$
	O9–H9o···O5	1.80	2.764(7)	166	
	O10–H10o···O8	1.69	2.675(6)	175	$-1/2 + x, 1/2 - y, 1 - z$
	O11–H11o···O6	1.82	2.766(5)	160	$1 - x, 1/2 + y, 3/2 - z$
	O12–H12o···O3	1.72	2.705(6)	176	$2 - x, 1/2 + y, 3/2 - z$
	O13–H13o···O11	1.71	2.688(6)	170	$3/2 - x, 1 - y, 1/2 + z$
	O14–H14o···O15	1.72	2.679(6)	164	$1 + x, y, z$
	O15–H15o···O12	1.73	2.711(6)	173	$1 - x, -1/2 + y, 3/2 - z$
1c	O16–H16o···O10	1.76	2.726(5)	168	
	C51–H51···O12	2.50	3.251(7)	126	$1 - x, -1/2 + y, 3/2 - z$
	C7–H7c···π	2.63	3.91(1)	172	x, y, z
	C56–H56c···π	2.77	3.76(1)	153	$-1 + x, y, z$
	O1–H7···O3	1.80	2.767(1)	169	$x, 1/2 - y, -1/2 + z$
	O2–H8···O3	1.74	2.716(1)	170	$x, 3/2 - y, -1/2 + z$
	O3–H9···O1	1.89	2.771(1)	148	$1 - x, 1 - y, -z$
2	O3–H10···O2	1.85	2.803(1)	162	$x, -1 + y, z$
	C7–H6···π	2.66	3.550(2)	140	$x, 3/2 - y, 1/2 + z$
	O1–H3···O2	1.75	2.663(4)	153	$1/2 - x, 1/2 - y, 1 - z$
	N1–H4···O1	2.10	2.982(5)	145	$x, 1 - y, -1/2 + z$
	N1–H5···O2	2.00	2.982(5)	164	$x, -y, 1/2 + z$
	N2–H6···O1	2.12	2.976(5)	142	$x, 1 - y, -1/2 + z$
3	N2–H7···O2	1.94	2.947(4)	174	$x, -y, -1/2 + z$
	π···π		3.524		
	O1–H4···N2	1.93	2.913(3)	177	$x, -1 + y, z$
	O2–H5···N5	1.91	2.890(3)	171	$x, 1 + y, z$
	C2–H1···O1	2.49	3.508(3)	156	$1/2 - x, 1/2 + y, 1/2 - z$
	C10–H9···N6	2.49	3.525(4)	160	$x, 1 + y, z$
	C13–H10···N1	2.45	3.455(3)	154	$3/2 - x, -1/2 + y, 1/2 - z$
	C18–H11···N3	2.52	3.477(3)	147	$-x, 1 - y, -z$
	C16–N3···Car	3.199(3)	4.073(3)	133.8(2)	$1 - x, 1 - y, -z$
	C16–N3···Car	3.180(3)	4.173(3)	145.7(2)	$1 + x, y, z$
4	π···π		3.336		
	π···π		3.322		
	O1–H1a···O4	1.95	2.904(2)	162	$-1 + x, 1/2 - y, -1/2 + z$
	O1–H1b···O1	1.90	2.805(2)	151	$1 - x, -y, -z$
	O2–H2o···N2	1.97	2.952(3)	173	$-1 + x, 1/2 - y, -1/2 + z$
	O3–H3o···N1	1.77	2.751(2)	173	$x, 1/2 - y, 1/2 + z$
	O4–H4a···O1	1.96	2.904(2)	159	$1 + x, 1/2 - y, 1/2 + z$
	O4–H4b···O2	2.31	3.271(2)	166	$1 + x, y, z$
	C16–H16···π	2.42	3.422(2)	154	$2 - x, -1/2 + y, 1/2 - z$
	C18–H18···π	2.37	3.407(2)	160	x, y, z
5	O1–H7···N2	1.80	2.741(2)	158	$-1/2 + x, -y, 3/2 - z$
	O2–H8···N1	1.82	2.744(2)	155	$1/2 - x, y, 1/2 + z$

Table 2. Continued

structure	interaction	H···A (Å)	X···A (Å)	X–H···A (deg)	symmetry code
6	C9–H11···O1	2.38	3.405(2)	158	1/2 + x, -y, 1/2 – z
	C7–H8···π	2.73	3.681(2)	146	1/2 – x, y, -1/2 + z
	C8–H9···π	2.73	3.805(2)	172	1/2 – x, y, 1/2 + z
	O1–H1···O8	1.76	2.737(2)	170	1 + x, 1 + y, 1 + z
	O3–H2···O10	1.74	2.707(2)	166	
	O8–H8···N2	1.71	2.687(2)	171	–x, 1–y, 1–z
	O10–H10···N4	1.73	2.714(2)	177	
	N3–H3a···O1	2.18	2.985(2)	136	–1 + x, y, z
	N6–H6b···O3	2.00	2.937(2)	153	1 – x, 1 – y, 1 – z
	N3–H3b···N5	1.93	2.939(2)	174	x, y, 1 + z
7	N6–H6a···N1	2.09	3.099(2)	177	x, y, –1 + z
	C22–H21···π	2.53	3.395(2)	136	–x, 1 – y, 1 – z
	O1–H1o···N6	1.82	2.788(3)	166	
	O2–H2o···N2	1.79	2.764(3)	170	–1 + x, y, z
	N3–H3a···O4	2.09	3.006(3)	149	1 + x, y, z
	N3–H3b···N5	2.12	3.121(3)	173	1 – x, –y, –z
	O3–H3o···N10	1.85	2.823(4)	171	x, –1 + y, z
	N4–H4a···N1	2.05	3.047(3)	168	1 – x, –y, –z
	O4–H4o···N7	1.76	2.748(3)	178	x, –1 + y, z
	N9–H9a···O2	2.35	3.227(3)	144	x, 1 + y, z
8a	N9–H9b···N11	2.06	3.068(3)	179	1 – x, 2 – y, 1 – z
	N12–H12e···N8	2.00	3.007(3)	176	1 – x, 2 – y, 1 – z
	C23–H23a···π	2.90	3.657(3)	127	1 – x, 1 – y, 1 – z
	C31–H31c···π	2.72	3.759(3)	162	x, 1 + y, z
	C38–H38a···π	2.84	3.821(3)	150	x, y – 1, z
	O1–H1···N1	1.64	2.592(3)	163	
	O3–H3···O1	1.71	2.680(3)	168	–x, 1/2 + y, 1/2 – z
	C4–H4···O3	2.39	3.447(3)	166	–x, 2 – y, 1 – z
	C12–H12···O3	2.56	3.499(3)	145	
	C7–H7a···π	2.71	3.675(3)	149	–x, 1 – y, 1 – z
8b	O1–H4···O2	1.71	2.681(2)	169	1/2 – x, –1/2 + y, 1/2 – z
	O2–H5···N1	1.59	2.561(2)	170	–x, 1 + y, 1/2 – z
	C9–H10···π	2.58	3.579(2)	153	–x, y, 1/2 – z
	C14–H14A···π	2.91	3.737(2)	133	1/2 – x, –1/2 + y, 1/2 – z
	C15–H15···π	2.27	3.351(7)	173	–x, y, 1/2 – z
8c	O1–H1···N1	1.71	2.672(2)	166	1/2 – x, 1/2 + y, 1/2 – z
	C8–H8···O1	2.61	3.650(1)	162	1/2 – x, –1/2 + y, 1/2 – z
	O1–H1···N1	1.70	2.669(5)	169	
8d	O3–H3···N3	1.69	2.663(4)	171	1 – x, –y, 1 – z
	C18–H18···π	2.73	3.560(4)	133	1 – x, 1 – y, 1 – z
	C21–H21c···π	2.82	3.716(5)	140	1 – x, 1 – y, 1 – z
	π···π		3.507(1)		1 – x, –y, 1 – z
9a	π···π		3.628(1)		2 – x, 2 – y, 2 – z
	O1–H1···N1	1.75	2.728(4)	174	1 – x, –y, 1 – z
	O3–H3···N2	1.75	2.728(4)	172	2 – x, 2 – y, 2 – z
	π···π		3.507(1)		1 – x, –y, 1 – z
9b	π···π		3.628(1)		2 – x, 2 – y, 2 – z
	O1–H1o···N1	1.70	2.675(3)	171	
	O3–H3o···N2	1.71	2.692(2)	176	
	O5–H5a···O10	1.83	2.798(3)	168	x – 1/2, 1/2 – y, z
	O5–H5b···O1	1.75	2.711(3)	163	x, y, 1 + z
	O8–H8o···O3	1.75	2.726(3)	172	
	O10–H10o···O5	1.65	2.606(3)	163	
	C2–H2···N1	2.54	3.296(3)	126	
	C25–H25···O8	2.49	3.260(3)	127	–x, 1 – y, z – 1/2
	C7–H7c···π	2.87	3.613(3)	126	x – 1/2, 1/2 – y, z
9c	C14–H14a···π	2.79	3.867(3)	176	1/2 + x, 1/2 – y, z

Table 2. Continued

structure	interaction	H···A (Å)	X···A (Å)	X–H···A (deg)	symmetry code
10a	O1–H7···N3	1.87	2.828(2)	165	
	O2–H8···N5	1.79	2.762(2)	169	
	N2–H13···O4	2.16	3.162(2)	170	$1 - x, 2 - y, 1 - z$
	N2–H14···O6	1.90	2.905(2)	173	$-x, 1 - y, 1 - z$
	N4–H19···O5	2.00	2.991(2)	168	$1 - x, 1 - y, 1 - z$
	N4–H20···N7	2.00	2.921(3)	151	$x, y - 1, z$
	N6–H25···N1	2.00	2.939(3)	155	
	N6–H26···O4	1.96	2.960(2)	172	$1 - x, 1 - y, 1 - z$
	N8–H31···O3	1.92	2.926(2)	179	$x, 1 - y, 1 - z$
	N8–H32···O5	2.11	3.116(2)	172	$1 - x, 1 - y, 1 - z$
	C4–H3···N5	2.50	3.264(3)	126	
	C12–H12···O1	2.47	3.517(3)	162	$x, 1 + y, z$
	C24–H24···O2	2.46	3.255(3)	129	$1 + x, y, z$
	C26–H27···O5	2.49	3.444(3)	146	$1 - x, 1 - y, 1 - z$
	C18–H16···π	2.67	3.716(2)	162	$1 - x, 1 - y, -z$
	C30–H30···π	2.88	3.886(2)	154	x, y, z
10b	O2–H2···O7	1.65	2.62(1)	173	$2 - x, 1 - y, -z$
	O1–H1c···N3	1.84	2.74(1)	151	$1 - x, 1 - y, -z$
	N2–H2a···N5	2.00	2.99(1)	167	$x - 1, y, z$
	N2–H2b···O4	2.00	3.01(1)	175	$1 - x, 1 - y, 1 - z$
	N4–H4a···N7	1.95	2.94(1)	165	
	N4–H4b···O3	1.98	2.94(1)	160	$1 - x, 1 - y, 1 - z$
	N6–H6a···O3	2.06	3.01(1)	156	$1 - x, 1 - y, 1 - z$
	N6–H6b···O5	2.03	2.95(1)	150	$1 - x, -y, 1 - z$
	O7–H7d···N1	1.82	2.78(1)	165	$1 + x, y, z$
	O7–H7e···O1	1.92	2.73(1)	137	$1 - x, 1 - y, -z$
	N8–H8a···O4	2.07	3.01(1)	154	$1 - x, 1 - y, 1 - z$
	N8–H8b···O6	1.88	2.88(1)	169	$-x, -y, 1 - z$
	C20–H20···O3	2.39	3.26(1)	137	$1 - x, 1 - y, 1 - z$
	C26–H26···O4	2.31	3.28(1)	148	$1 - x, 1 - y, 1 - z$
	C12–H12···π	2.47	3.48(1)	155	$x - 1, y, z$
11	O1–H4···N1	1.75	2.731(2)	175	$x, 1 - y, -1/2 + z$
	O2–H5···N3	1.87	2.840(2)	169	$x, 1 - y, -1/2 + z$
	N2–H13···O4	2.02	2.941(2)	150	$x, 1 + y, z$
	N2–H14···O4	2.11	3.068(2)	158	$1/2 - x, 3/2 - y, -z$
	N4–H19···O1	1.95	2.894(2)	154	$x, 1 + y, z$
	N4–H20···O3	1.90	2.901(2)	173	$1/2 - x, 3/2 - y, -z$
	C4–H2···N3	2.55	3.391(2)	133	$x, 1 - y, -1/2 + z$
	C11–H12···O1	2.41	3.363(2)	146	$x, 1 + y, z$
	C18–H18···O2	2.37	3.402(3)	159	$-x, 1 - y, -z$
12	O1–H1···N1	1.72	2.674(1)	163	
	N1–H1n···O1	2.28	3.111(2)	139	$1/2 - x, 1/2 - y, -z$
13	O1–H7···O2	1.76	2.736(1)	169	$3/2 - x, 1/2 + y, 1/2 - z$
	O2–H8···N1	1.78	2.747(1)	166	
	C2–H1···O1	2.60(1)	3.533(3)	162	
	π···π	—	3.420		$1 - x, 1 - y, -z$
14a	O1–H1···N4	1.77	2.751(3)	176	$1 - x, 1/2 + y, 1/2 - z$
	O3–H3···N1	1.87	2.851(3)	173	
	C11–H11···O1	2.34	3.288(4)	145	$x, 1/2 - y, 1/2 + z$
	C16–H16···O1	2.40	3.309(3)	140	$2 - x, -1/2 + y, 1/2 - z$
	C8–H8···π	2.78	3.584(3)	131	$-1 + x, y, z$
	C20–H20···π	2.92	3.948(3)	158	$1 - x, -y, -z$
	π···π		3.381		
	π···π		3.333		
14b	O1–H1···O8	1.84	2.789(4)	161	$1 + x, 1 + y, 1 + z$

Table 2. Continued

structure	interaction	H···A (Å)	X···A (Å)	X–H···A (deg)	symmetry code
15	O3–H3···N1	1.90	2.854(5)	164	$1 - x, 1 - y, 1 - z$
	O8–H8···N2	1.85	2.823(5)	170	$1 - x, 1 - y, -z$
	O10–H10···O3	1.84	2.816(4)	174	
	C17–H17···O1	2.35	3.351(6)	153	$x, y, -1 + z$
	C20–H20···O10	2.41	3.300(6)	138	
	$\pi \cdots \pi$		3.612		$1 - x, 1 - y, 1 - z$
	O1–H1···N4	1.83	2.810(4)	176	
	O3–H3···N1	1.78	2.753(3)	170	
	C7–H7A···N3	2.75	3.720(2)	173	$1 - x, 2 - y, 1 - z$
	C16–H16··· π	2.76	3.683(4)	142	$x, -1 + y, z$
16	$\pi \cdots \pi$		3.412		
	O1–H1o···N2	1.81	2.736(2)	156	
	O2–H2o···N3	2.08	2.901(3)	139	$x, -1 + y, z$
	O2–H2o···N4	2.32	3.132(3)	140	$x, -1 + y, z$
	C10–H10···O2	2.45	3.486(3)	159	$x, 1 + y, z$
	C15–H15··· π	2.70	3.618(3)	142	$x, 1/2 - y, 1/2 + z$
	C25–H25··· π	2.48	3.530(3)	163	$1 - x, 1 - y, 1 - z$
$\pi \cdots \pi$			3.447		

four cyano acceptors, only two are involved in the formation of strong O–H···N hydrogen bonds. The other two cyano N-atoms forms weak C–H···N interactions with the aryl H-atoms (Figure 3d). These weak interactions along with $\pi \cdots \pi$ and $C\equiv N^{(\delta-)} \cdots CAr^{(\delta+)}$ interactions hold the tetramers together in the 3-D arrangement (Table 2).

Orcinol–4-Cyanopyridine 2:1 Co-Crystal (4). Orcinol and 4-cyanopyridine (2:1) co-crystallize from MeCN in the space group, $P2_1/n$. One of the hydroxy groups of the orcino molecules is disordered so that the resultant conformation could be either *anti-anti* or *syn-anti*. The two symmetry independent orcino molecules form O–H···O hydrogen bonded chains (Figure 3e), and the 4-cyanopyridine molecules act as linkers between these chains interacting at the one end through the pyridine N-atom and at the other through the cyano N-atom with O–H···N hydrogen bonds (Figure 3f). The resorcinol–4-cyanopyridine co-crystal reported by Bis et al.¹⁷ obtained from the same solvent adopts an entirely different packing (*synthon A*) driven purely by the *anti-anti* orcino conformer **B** rather a mixture of conformers as seen in co-crystal (4). Such *anti-anti* packing is sampled in orcino co-crystallization experiments but with other co-formers, 4-(*N,N'*-dimethylamino)pyridine (**8c**) and quinoxaline (**14a**) discussed later in this paper.

Orcinol–Hexamethylenetetramine 1:1 Co-Crystal (5). The title compound forms a 1:1 adduct with hexamethylenetetramine (HMTA, hexamine, urotropin). The space group is $Pccn$ and $Z' = 1$. A discrete 4-membered cyclic assembly is found that consists of two HMTA held from either sides by two orcino molecules (*anti-anti* conformer) with four O–H···N hydrogen bonds (Figure 3g). Two of the four potential N-atom acceptors form O–H···N hydrogen bonds. These tetramer units are stacked in layers held together by C–H··· π interactions between the C–H donors of HMTA and the aromatic ring (Table 2). The HMTA co-crystals with resorcinol (CSD refcode RSHMTA) and methyl 3,5-dihydroxybenzoate (CSD refcode FEQXEF) adopt zigzag chain topologies driven by *syn-anti* conformations of the respective 1,3-dihydroxybenzenes.

Orcinol–2-Aminopyrimidine 1:1 Co-Crystal (6). Orcinol forms a 1:1 co-crystal with 2-aminopyrimidine in the space group $P\bar{1}$ with $Z' = 2$. One orcino molecule is *syn-syn* conformation and other is *anti-anti* and the two conformations alternate in a O–H···O hydrogen bonded chain (Figure 4a). The 2-aminopyrimidine molecules retain their robust N–H···N dimer motif and interlink the 1-D chains with N–H···O (with *anti-anti*) and O–H···N (with *syn-syn*) hydrogen bonds, respectively (Figure 4b, Table 2).

Orcinol–2-Amino-4,6-dimethylpyrimidine 1:2 Co-Crystal (7). Orcinol and 2-amino-4,6-dimethylpyrimidine crystallize in a 1:2 ratio in the space group $P\bar{1}$ with $Z' = 2$. Similar to orcino–2-aminopyrimidine, **6**, the robust N–H···N dimer motif is preserved. However, the overall structure of **7** was found to be different from that of co-crystal **6**. Co-crystal **7** has a six-membered cyclic assembly in which the two 2-aminopyrimidine N–H···N dimer units are enclosed by two *anti-anti* orcino molecules with O–H···N hydrogen bonds (Figure 4c). This hexamer is analogous to the cyclic assembly seen in orcino–HMTA. Two sets of such discrete cyclic assemblies are generated by the four symmetry independent molecules of 2-amino-4,6-dimethylpyrimidine. These sets are interlinked with N–H···O hydrogen bonds between the free amino N–H groups and the hydroxyl O-atoms (Figure 4d).

Orcinol–4-(*N,N'*-dimethylamino)pyridine 1:1 Co-Crystal (8a). A total of four co-crystal forms of orcino–4-(*N,N'*-dimethylamino)pyridine (**8a** through **8d**) were obtained from different crystallization experiments (Supporting Information). A 1:1 co-crystal was obtained from acetonitrile in space group $P2_1/c$. The orcino molecules are *syn-anti* and form 1-D chains of O–H···O hydrogen bonded molecules related by a c_1 screw axis. The 4-(*N,N'*-dimethylamino)pyridine molecule is pendant from these chains by means of O–H···N hydrogen bonds. These 1-D chains are held together with short centrosymmetric C–H···O dimers formed between orcino molecules of two neighboring chains (Figure 5b). This pattern extends in the third dimension with weak C–H···O and C–H··· π interactions.

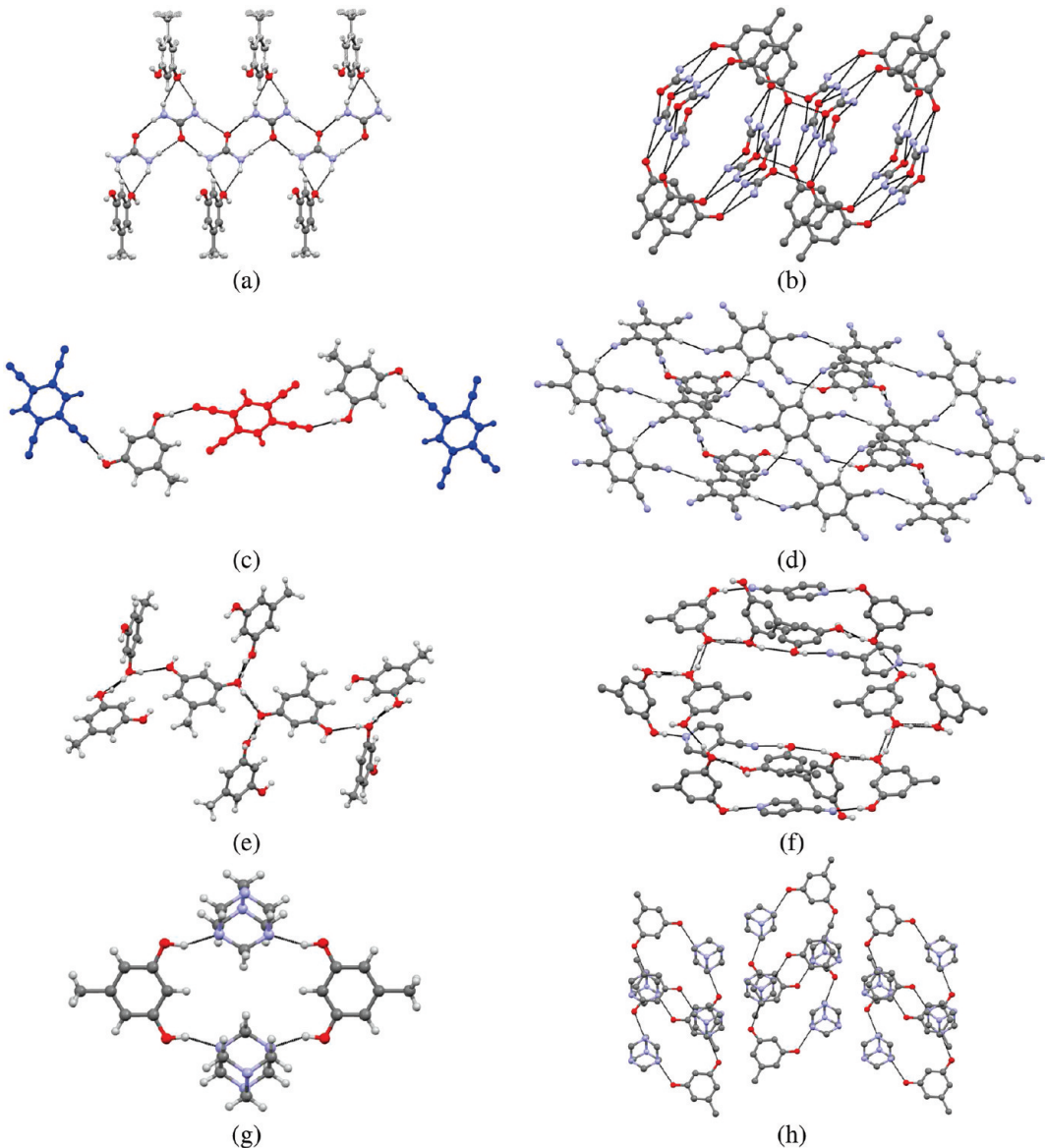


Figure 3. Crystal packing in orcinol co-crystals (a–b) urea, **2**; (c–d) 1,2,4,5-tetracyanobenzene, **3**; (e, f) 4-cyanopyridine, **4** and (g, h) hexamethylenetetramine, **5**.

Orcinol–4-(*N,N'*-Dimethylamino)pyridine 1:1 Co-Crystal Chloroform Solvate (8b**).** Co-crystallization experiments in chloroform resulted in the isolation of a solvate of the 1:1 co-crystal of orcinol and 4-(*N,N'*-dimethylamino)pyridine in space group $C2/c$. The orcinol molecule is *syn-anti*. A disordered chloroform molecule sits on a special position. The 1-D chain of $O-H \cdots O$ hydrogen bonds is retained as in the solvent-free **8a**. Adjacent chains slide in opposite directions to accommodate solvent molecules, and this breaks the centrosymmetric $C-H \cdots O$ dimer found in the solvent-free **8a** (Figure 5d).

Orcinol–4-(*N,N'*-Dimethylamino)pyridine 1:2 Co-Crystal Form I (8c**).** A 1:2 co-crystal of orcinol–4-(*N,N'*-dimethylamino)pyridine was obtained from isopropyl acetate in space group $C2/c$ with $Z' = 0.5$. This orcinol molecule is bisected by a 2-fold axis and adopts the *anti-anti* conformation. Molecules are arranged in a V-shaped trimer motif consisting of two pyridine molecules and one orcinol molecule linked with $O-H \cdots N$ hydrogen bonds (Figure 5e).

Orcinol–4-(*N,N'*-Dimethylamino)pyridine 1:2 Co-Crystal Form II (8d**).** A polymorphic form II of this 1:2 co-crystal was obtained from nitromethane. Note that once again nitromethane seems to be an effective solvent for the generation of a new polymorph. Form II, **8d**, crystallizes in space group $P\bar{1}$, with $Z' = 1$. The orcinol molecule adopts a *syn-syn* conformation in contrast to the *anti-anti* conformation in **8c**, but as in **8c** the molecules form an alternating array of trimers packed in a linear fashion (Figure 5g,h). These layers interact through weak centrosymmetric $C-H \cdots O$ dimers.

The structural variability in co-crystals of orcinol with mono-N-acceptor systems is nicely exemplified by the observed polymorphs and pseudopolymorphs **8a–d** obtained in the orcinol–4-(*N,N'*-dimethylamino)pyridine system. Three different packing arrangements driven by *syn-anti*, *anti-anti*, and *syn-syn* conformers of orcinol were isolated by a mere change in the crystallizing conditions. Co-crystals directed by orcinol *syn-anti*, **8a** and *anti-anti*, **8c** conformers do not show much variation in

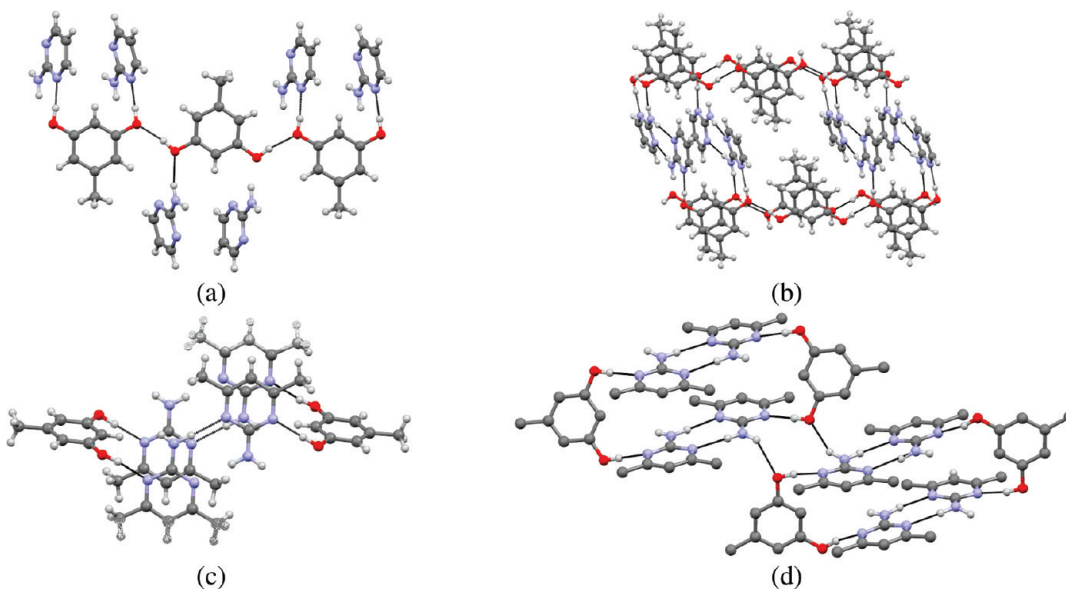


Figure 4. Crystal packing in orcinol co-crystals with (a, b) 2-aminopyrimidine, 6 and (c, d) 2-amino-4,6-dimethylpyrimidine, 7.

terms of crystal density, 1.232 and 1.231 g/cm³. However, a slightly better packing coefficient (KPI) of 70.1% was obtained for **8c** than in **8a**, 68.5%. The third packing variation, **8d** directed by the least stable *syn-syn* conformer A was found to have the lowest density and packing coefficient among these (density, 1.198 g/cm³; KPI, 65.1% see Supporting Information, Table S2).

Orcinol–Acridine 1:2 Co-Crystal (9a). Orcinol forms a 1:2 co-crystal with acridine and crystallizes (from ethyl acetate) in the space group, $P\bar{1}$. The orcinol molecule adopts a *syn-syn* conformation and is bound with two molecules of acridine through O–H···N hydrogen bonds (Table 2). These trimer units are arranged in linear stacks. The aromatic rings of the adjacent antiparallel stacks intercalate themselves in between these stacks with $\pi \cdots \pi$ interactions (Figure 6b).

Orcinol–Acridine 1:1 Co-Crystal Hydrate (9b). A hydrated orcinol–acridine co-crystal was obtained from chloroform and crystallizes in space group $Pna2_1$ with $Z' = 2$. The two symmetry independent orcinol molecules adopt *anti-anti* and *syn-anti* conformations. Both acridine molecules are bound to the *anti-anti* conformer with O–H···N hydrogen bonds (Table 2). The *syn-anti* conformer of orcinol interacts with water and with the *anti-anti* molecule forming ring topology $R_8^8(32)$. There are three water molecules and five orcinol molecules (two *anti-anti* and three *syn-anti*) in this eight-membered supramolecular ring (Figure 6d).

Orcinol–Nicotinamide 1:4 Co-Crystal (10a). Orcinol forms a 1:4 molecular complex with nicotinamide and crystallizes (from ethyl acetate) in the space group, $P\bar{1}$. The nicotinamide molecules form amide–amide N–H···O homodimers (Figure 7a). The free N–H groups on the either side of the dimer units interact with the carbonyl O-atoms of adjacent dimers on one side and with the free pyridine nitrogen atoms on the other side (Table 2). This results in a linear tape of nicotinamide molecules but one which is distinct from the classical amide tape formed by 1° amides. The orcinol molecules (*anti-anti* conformer) clip two parallel tapes with the help of O–H···N hydrogen bonds formed to the pyridine N-atoms of the nicotinamide (Figure 7b).

Orcinol–Nicotinamide 1:4 Co-Crystal Hydrate (10b). A hydrate of orcinol–nicotinamide 1:4 co-crystal was obtained

from ethanol in the space group, $P\bar{1}$. The free amide N–H groups on the either side of the dimer unit interact with the carbonyl O-atom of the adjacent dimer unit on one side and with the free pyridine nitrogen atom on the other side from the neighboring layer (Table 2). The orcinol molecules are *anti-anti* and act as clips joining two adjacent chains with the O–H···N hydrogen bonds with the pyridine nitrogen at one end and through water bridged interactions from the other (Figure 7c,d).

Orcinol–Isonicotinamide 1:2 Co-Crystal (11). Unlike orcinol–nicotinamide 1:4 co-crystal (10), orcinol forms a 1:2 co-crystal with isonicotinamide in the space group $C2/c$. However, the amide homodimer motif is retained in the co-crystal (Figure 7e). The orcinol molecule is *anti-anti* and forms a six-membered cyclic assembly similar to that seen in the case of aminopyrimidine co-crystals (6 and 7).

Orcinol–Piperazine 1:2 Co-Crystal (12). Orcinol and piperazine co-crystallize in the space group, $C2/c$ with $Z' = 0.5$. Orcinol adopts an *anti-anti* conformation. The nitrogen atoms of the piperazine ring act both as hydrogen bond donor (N–H) and as an acceptor forming co-operative N–H···O and O–H···N hydrogen bonds with orcinol. Orcinol and piperazine assemble in a 1-D sinusoidal wave pattern of O–H···N hydrogen bonds along the *c*-axis as shown in Figure 8b. The free NH group of piperazine links these ribbons in the perpendicular direction through O–H···N hydrogen bonds.

Orcinol–Pyrazine 2:1 Co-Crystal (13). Orcinol forms a 2:1 co-crystal with pyrazine in space group, $P21/n$ with $Z' = 0.5$. In this structure, orcinol is *syn-anti* and forms a chain of O–H···O hydrogen bonds between 2₁ related molecules. The pyrazine acts as a linker between neighboring orcinol chains in the second dimension. These interactions are complemented by symmetrical orcinol–orcino C–H···O dimers (Figure 8) in the third dimension leading to the formation of a cross-linked 3-D network of hydrogen bonds.

Orcinol–Quinoxaline 1:2 Co-Crystal (14a). Co-crystal 14a (obtained from ethyl acetate) takes the space group $P2_1/c$ with $Z' = 1$. The orcinol molecule is *anti-anti* and forms O–H···N hydrogen bonds of similar geometry with the two symmetry independent quinoxaline molecules forming discrete trimer

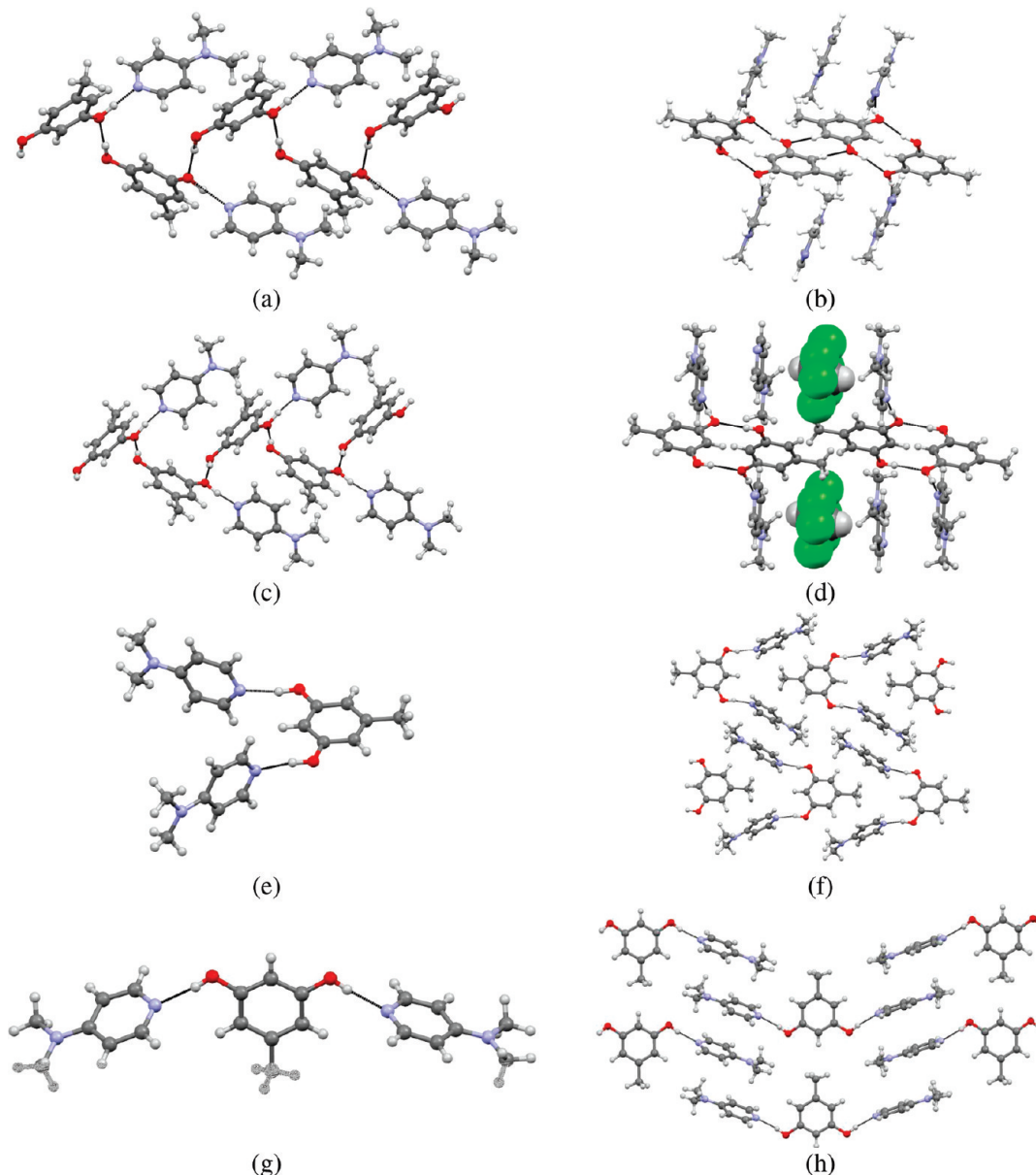


Figure 5. Crystal packing in the orcinol co-crystals with 4-(*N,N'*-dimethylamino)pyridine (a, b) 1:1 co-crystal, 8a; (c, d) chloroform solvate of 1:1 co-crystal, 8b; (e, f) 1:2 co-crystal form I, 8c and (g, h) 1:2 co-crystal form II, 8d.

units. Only one of the nitrogen atoms of the quinoxaline molecules is involved in the hydrogen bonding with orcinol. The unbound nitrogen atom is involved in the formation of weak C–H···N bonds with the other quinoxaline molecule (Figure 9). The trimer unit assembles along the *b*-axis with stacked quinoxaline molecules and weak C–H···O bonds formed between orcinol and quinoxaline molecules (Table 2).

Orcinol–Quinoxaline 2:1 Co-Crystal (14b). A 2:1 co-crystal of orcinol–quinoxaline (14b) was obtained from diethyl ether. Co-crystals 14a and 14b exhibit different stoichiometries and so may be considered to be pseudopolymorphs.¹⁸ The second form crystallizes in the space group *P*1 with *Z'* = 1. Both symmetry independent orcinol molecules adopt the *syn-anti* conformation. In contrast to 14a, both the N-atoms of the quinoxaline molecule are involved in hydrogen bonding. Analogous to 13, the orcinol molecules in 14b are held by O–H···O hydrogen bonds and

the two N-atoms of the heterocyclic ring act as a bidentate linker between adjacent chains by forming O–H···N bonds (Figure 9). Additionally, the C–H groups on the benzene ring of quinoxaline form short C–H···O interactions with orcinol. The third dimension is extended with long C–H···O interactions.

Orcinol–Phenazine 1:2 Co-Crystal (15). Orcinol and phenazine co-crystallize in the space group *P*1 in a 2:1 ratio. Orcinol adopts a *syn-syn* conformation and holds the two phenazine molecules from either side by O–H···N hydrogen bonds forming T-shaped trimer units. The phenazine rings of the two adjacent trimer units (related by center of inversion) are held together by $\pi \cdots \pi$ interactions with an interplanar distance of 3.46 Å and a long C–H···N interaction (Table 2). These inversion related trimer units form a two-dimensional (2-D) layered structure along the plane (0, -1, 2). The phenazine and

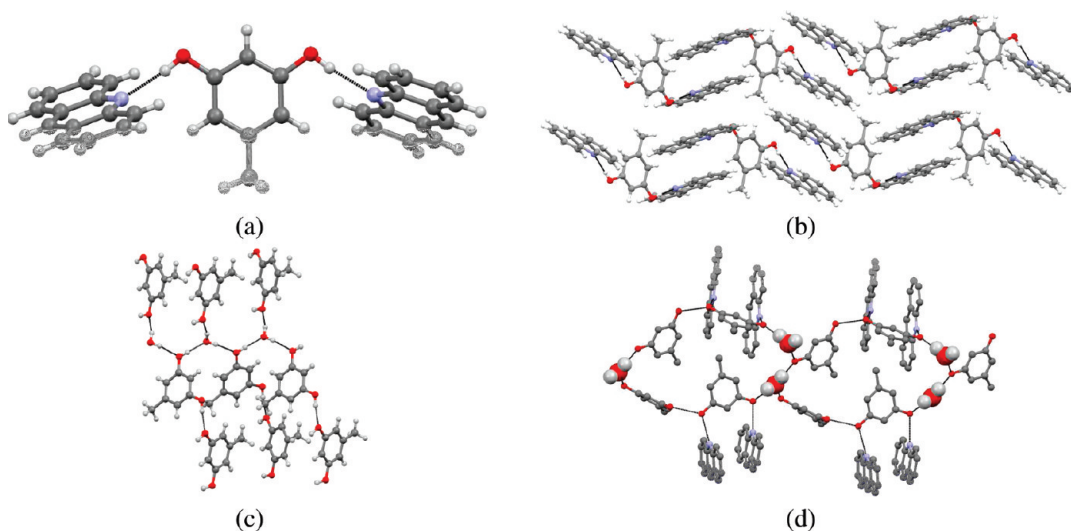


Figure 6. Crystal packing in orcinol co-crystal with acridine (a, b) 1:2 co-crystal, **9a** and (c, d) 1:1 co-crystal hydrate, **9b**.

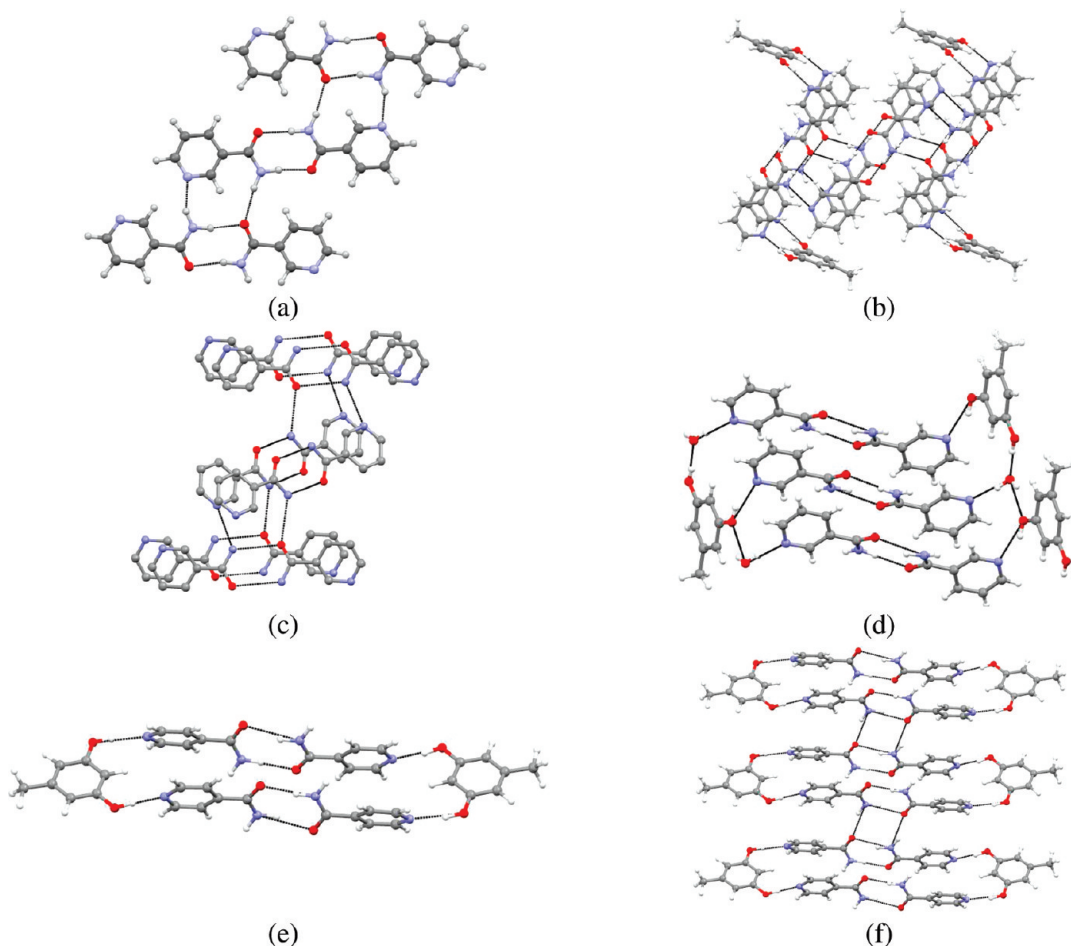


Figure 7. Crystal packing in orcinol (a, b) 1:4 nicotinamide co-crystal, **10a**; (c, d) 1:4 nicotinamide co-crystal hydrate, **10b** and (e, f) isonicotinamide co-crystal, **11**.

orcinal in adjacent layers interact with C–H \cdots π interactions (Figure 10).

Orcinal–1,10-Phenanthroline 1:2 Co-Crystal (16). Orcinal forms a 1:2 co-crystal with phenanthroline in the space group

$P2_1/c$ and with $Z' = 1$. The orcinol is *syn-syn*. As expected, the main interaction is an O–H \cdots N hydrogen bond that creates trimer synthon D similar to that found in the co-crystals **8d**, **9b**, and **15**. These trimer units are arranged about centers of

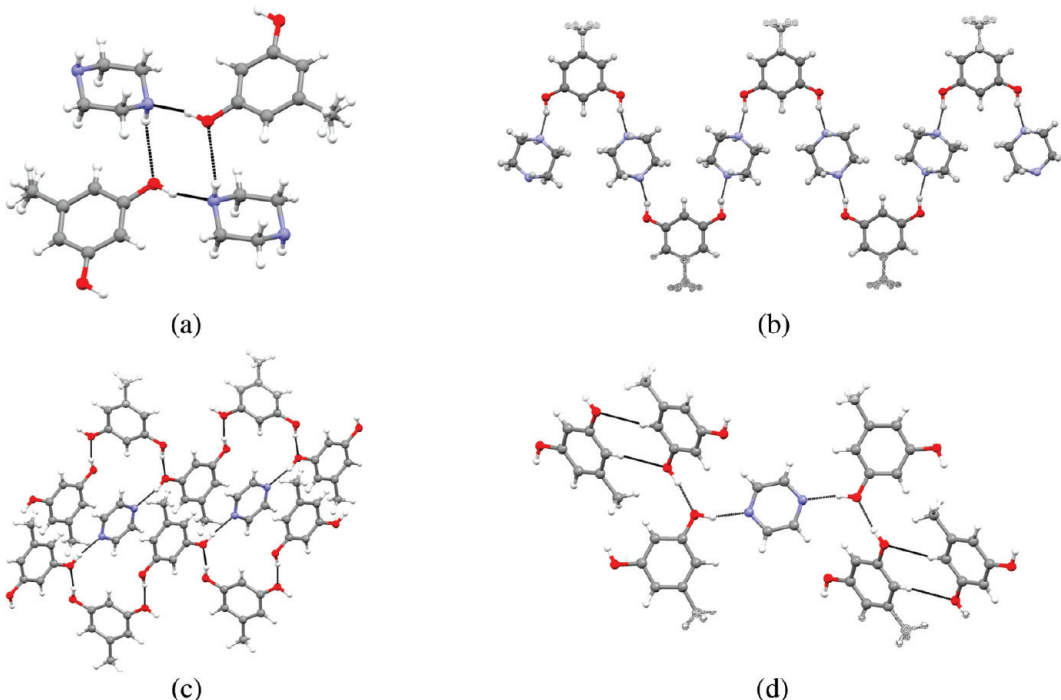


Figure 8. Crystal packing in the orcinol co-crystals with (a, b) piperazine, **12** and (c, d) pyrazine, **13**.

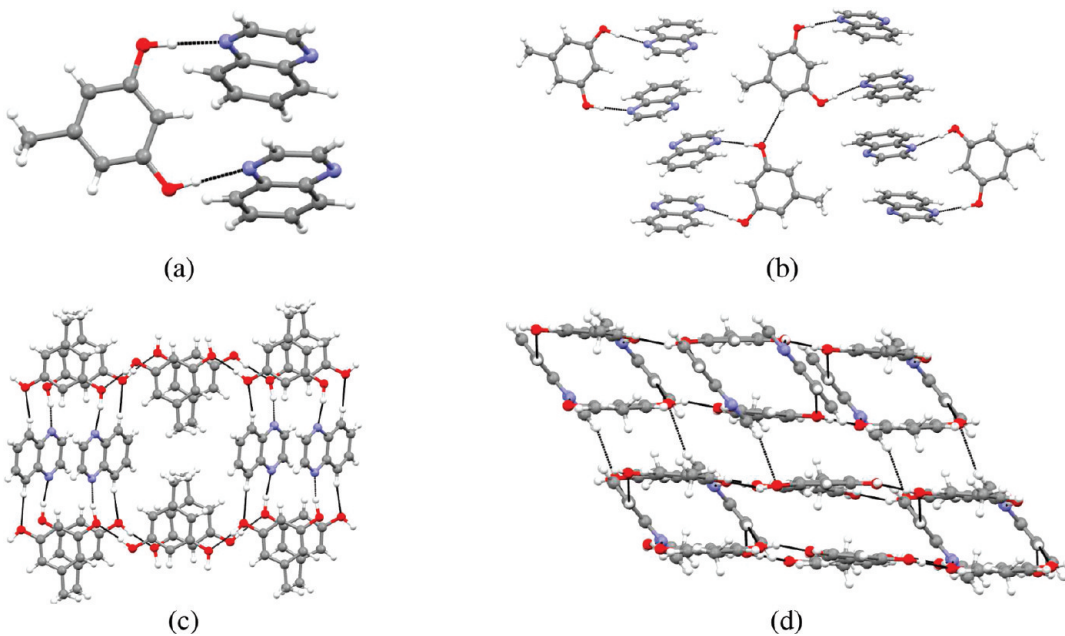


Figure 9. Crystal packing in orcinol co-crystals with quinoxaline (a, b) 1:2 co-crystal, **14a**; (c, d) 2:1 co-crystal, **14b**.

inversion and are held together by short C–H \cdots π interactions between the phenanthroline rings. Stacking is observed between parallel phenanthroline rings of adjacent centrosymmetric hexamer units with the distance between the planes being 3.39 Å (Figure 10).

■ DISCUSSION

Orcinol is a simple molecule but it can easily invoke a conflict between intermolecular interactions and close packing because it

takes multiple conformations. Moreover, these conformations are equienergetic and so their relative distribution is easily affected by small changes in the crystallization conditions. The high Z' values observed in both anhydrous forms of orcinol (**1a** and **1b**) are of particular interest. Isolation of the high Z' form II (**1b**; $Z' = 8$) of orcinol indicates a situation where there is an equal distribution of all the three conformers of orcinol, resulting in the nucleation of a crystal form with two molecules each from the *syn-syn*, *syn-anti*, *anti-syn*, and *anti-anti* conformers. However,

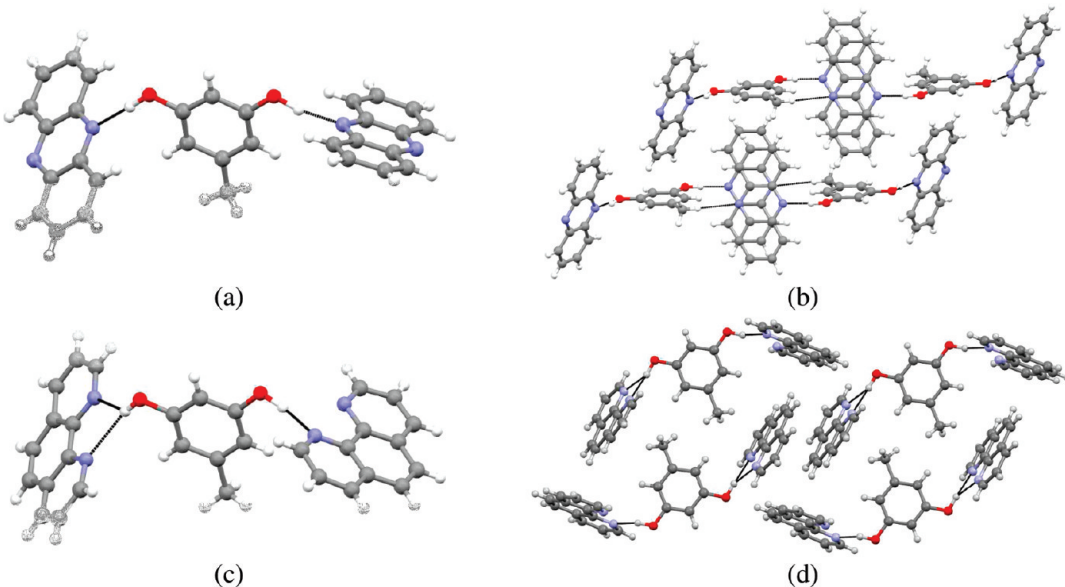
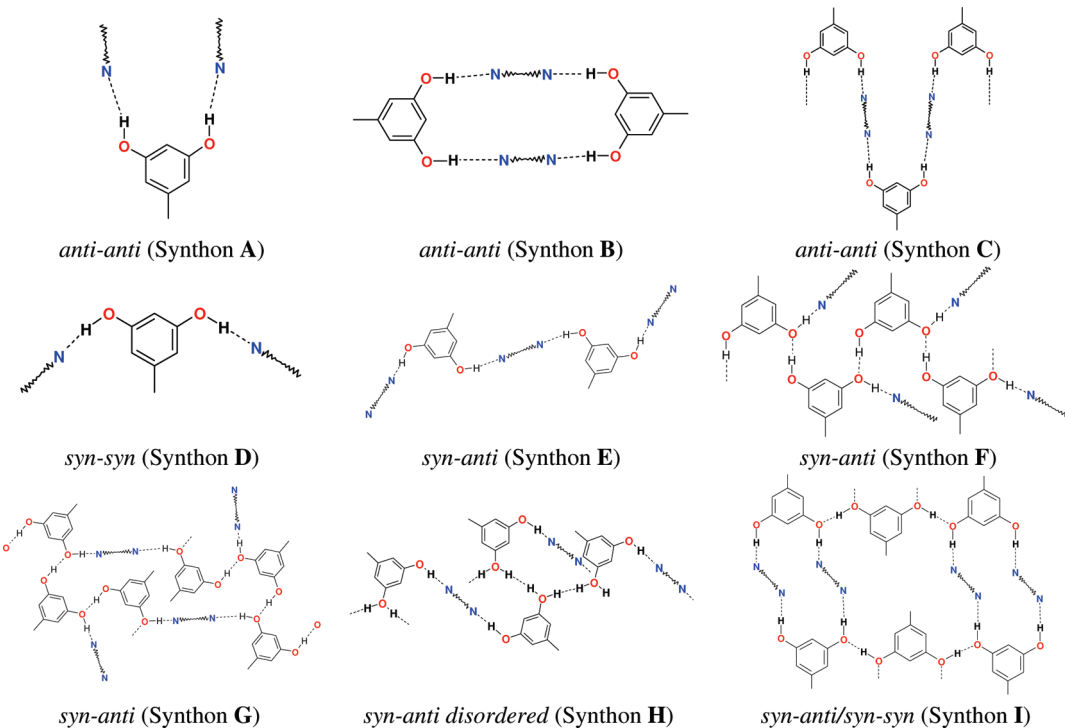


Figure 10. Crystal packing in the orcinol co-crystals with (a, b) phenazine, **15**; (c, d) 1,10-phenanthroline, **16**.

Scheme 3

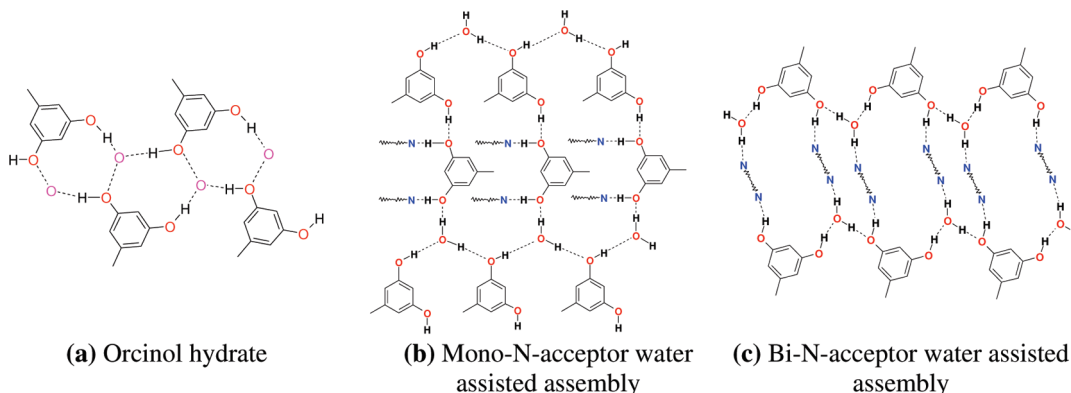


such a situation is very difficult to predict and represents a random event of low probability. We were unable to obtain this form again despite several attempts.

The extensive orcinol co-crystallization study performed here with various nitrogen containing co-crystal formers casts some light on the available crystallization pathways originating from these orcinol conformations. There are two earlier reports on the orcinol co-crystals with N-acceptors, 2,5-bis((4-pyridyl)ethynyl) thiophene (CSD refcode LEDBEC) and 1,4-diazabicyclo-(2.2.2)octane (CSD refcode PAJFAI). In both cases, the orcinol

molecule has the *anti-anti* conformation B but it adopts different packing modes, a discrete four-member cyclic assembly and a 1-D infinite zigzag chain of O—H \cdots N hydrogen bonds (discussed later in the manuscript, Scheme 3, Synthon B). Recently, Jones and co-workers¹⁹ have isolated a 1:1 co-crystal of orcinol with the antimalarial drug artemisinin, in which the orcinol molecule adopts the most stable *syn-anti* conformation. The drug molecules are held by O—H \cdots O hydrogen bonds formed between the orcinol OH group and the carbonyl oxygen of the artemisinin (similar to Synthon F, Scheme 3).

Scheme 4



The co-crystals of orcinol with nitrogen bases can be broadly divided into two main classes with mono- and bi-N-acceptor co-formers. Mono-N-acceptor co-formers preferably adopt one of three supramolecular geometries (synthons A, D, and F, Scheme 3). Synthons A and D are discrete 0-D supramolecular motifs where co-former molecules are held via O–H \cdots N hydrogen bonds in V- and M-shaped motifs. These synthons are also observed with bi-N-acceptor co-formers where only one of the N-atoms is involved in the recognition event. Synthon F is a 1-D supramolecular motif with co-former molecules pendant either side of an infinite chain of O–H \cdots O hydrogen bonds formed by *syn-anti* orcinol molecules. Overall, the bi-N-acceptor co-formers show more variability than the mono N-acceptor conformers, for example, 0-D (synthon A, B, D, and E), 1-D (synthon C), and 2-D interaction motifs (synthons G, H, and I). Also, they show examples wherein orcinol adopts more than one type of conformation in the same co-crystal (4 and 6).

Crystallization conditions can greatly affect solubility, nucleation, growth rates, and crystal habit. The crystallization and formation of polymorphic modifications will be a function of the applied conditions (solvent(s), temperature, crystallization technique) as well as the nature and concentration of co-crystal former used (see crystallization matrices given in the Supporting Information). In many cases, co-crystal stoichiometry is controlled partly by the chosen co-former ratios (8, 10, 14, Supporting Information). It is apparent from the crystal structures of orcinol with 4-(*N,N'*-dimethylamino)pyridine (**5a**–**5d**) that both solvent and co-former ratios seem to play a role in the investigated system. The amount of co-crystal former taken is not always a critical factor during co-crystallization experiments.

Water-Assisted Multicomponent Assemblies. A few hydrate structures were also observed during the crystallization and co-crystallization experiments with orcinol. Unlike other solvents water always has a specific role to play in the molecular organization.²⁰ Orcinol tends to mostly crystallize as a hydrate under normal conditions. In orcinol monohydrate (**1c**) water selectively stabilizes the most stable *syn-anti* conformer in an extensive hydrogen bonding network (Scheme 4). However, in the anhydrous form I (**1a**) this is achieved at the cost of $Z' = 2$. A more chaotic situation is observed in the form II structure that ends up with an even higher value of $Z' = 8$.

Additionally, two more hydrated structures were observed for acridine and nicotinamide co-crystals (**9b** and **10b**), being representative of co-crystal hydrates of mono- and bi-N-acceptor

Table 3. Relative Distribution of Supramolecular Synthon Geometries in Orcinol Co-Crystals

conformer ^a	mono-N-acceptors			bi-N-acceptors							total
	A	D	F	A	D	B	C	E	G	H	
syn-syn			2			2					4
anti-anti	1				1	4	1				7
syn-anti				2			1	2			5
mixed/disordered								1	1	2	
total	1	2	2	1	2	4	1	1	2	1	18

^a Urea, orcinol polymorphs, and hydrated structures are not included.

co-crystal assemblies. The crystal patterns are shown in Scheme 4. The isolation of orcinol-acridine hydrate can be related to either of two events. First, it could be that the inclusion of water in the crystal structure helps in the extension of a 0-D assembly (synthons C and D, Scheme 3) commonly observed in the mono-N-acceptor co-crystals (**8c**, **8d**, **9a**, **14a**, **15**, **16**) en route to a relatively more stable 2-D packing motif. Alternatively, one could relate it to the possibility of simultaneous growth of a nucleus consisting of orcinol–mono-N-acceptor trimer unit (Synthon A, Scheme 3), and the *syn-anti* conformer of orcinol assisted by the presence of water during the crystallization event. The representative example for a bi-N-acceptor type water assisted co-crystal assembly is obtained for the orcinol–nicotinamide co-crystal hydrate (**10b**). This presents a special case in which inclusion of water in the crystal structure provides an alternative packing mode with cross-linked layers of *anti-anti* molecules (synthon B) assisted by water molecules. This possibly provides a relatively more favorable growth unit than in the anhydrous form.

Relative Distributions of Various Motifs. An understanding of synthon distribution can provide useful insights in terms of crystal growth kinetics. For example, co-crystallization experiments of orcinol with bi-N-acceptor systems preferentially lead to the discrete cyclic synthon B with the *anti-anti* conformer. Such motifs are quite common for other members of the 1,3-dihydroxybenzene family. The relative occurrences of various supramolecular motifs observed in the co-crystallization experiments are given in Table 3. The synthons originating from the most stable *syn-anti* conformation constitute the second most preferred arrangement for both mono- and bi-N-acceptor systems.

■ CONCLUSIONS

Various crystallization and co-crystallization pathways for the orcinol molecule have been studied with high throughput crystallization. Two polymorphs and a hydrated form (pseudopolymorph) have been characterized. Eight different packing modes for bi-N-acceptor systems and three for the mono-N-acceptor systems have been identified for orcinol co-crystals. Additionally, a few new packing modes were observed in the hydrates. Isolation and characterization of each of these forms establishes the idea of the structural landscape. Further studies on the control and optimization of crystallization conditions will help in devising future crystal engineering strategies. The landscape is defined by the possible, and nearly equienergetic, crystal forms that are available to a molecule. Normally, the landscape is defined by the polymorphs of a compound and selected solvates (pseudopolymorphs). Examination of a large number of co-crystals of orcinol enables the crystal engineer to sample the conformational space available to the molecule. A decent idea of the landscape would be obtained if one chooses a sufficiently large number of crystal structures of related compounds. These structures should be similar enough so that they warrant selection within the same landscape and yet different enough that they sketch out a reasonable energy picture of the possible structures attainable in the system. If the number of data points is too small it is difficult to obtain characteristic features of the crystal structure landscape for the system of interest. Similarly, a very large data set may lead to a situation in which the correlation between the data points is lost. In this study we have not taken the conformational flexibility of the co-former N-bases into account. Such an extension will be very system specific and may result in the loss of generality due to an increase in the number of tunable parameters. The present availability of tabletop diffractometers that permit the acquisition and analysis of single crystal data for a crystal in the matter of a few hours greatly facilitates the process of exploring the structural landscape of any given molecule. Crystallography is used as a screening technique to examine a large number of crystals from each crystallization experiment. In this way, it is possible to identify the several cases of closely related structures that are possible for orcinol polymorphs, pseudopolymorphs, and co-crystals. Considering also that computer generated prediction of such crystal structures might not always be straightforward, high throughput crystallography is beginning to emerge as an important technique in the tool-kit of the crystal engineer.

■ APPENDIX: CRYSTAL STRUCTURE PREDICTION (CSP) OF HYDRATES

Crystal structure prediction (CSP) of solvates and hydrates²¹ is more difficult than CSP of other multicomponent systems. The

smaller size, the dual hydrogen bonding character of water, and its excellent ability to adapt according to the needs of the supramolecular environment make hydrates a very unique and difficult class of structures for the CSP exercise. This category has been recently introduced in the CSP blind test organized by the Cambridge Crystallographic Data Centre. The prediction of two new polymorphs (Molecule XXI, $Z' = 1$ and a $Z' = 2$ form)²² of gallic acid monohydrate was given one of the targets for the 5th CSP Blind test, 2010.²³ There are two already known polymorphs of gallic acid hydrate (CSD refcodes, KONTIQ and KONTIQ01). Depending on the relative orientation of three hydroxyl groups, a total of five conformations are possible for the gallic acid molecule (Scheme 5). The relative energies of these conformations follow the order Ic < Id < Ib < Ia < Ie (Supporting Information). Conformer C was found to be the most stable among these geometries.

CSP Strategy. A regular CSP will require exhaustive sampling of structures as the water molecule can be located anywhere around the molecule in each of these conformations. A restricted sampling of putative hydrate structures was obtained by selecting the most probable hydration sites identified as the negative potential regions in the molecular electrostatic potential maps (Supporting Information). The water molecule was placed at these selected regions and a rigid CSP was performed in each case. A total of 12 rigid CSP runs were performed and the top 50 low energy structures were merged together and re-ranked based on the most preferred conformations in the CSD. The information about the relative distribution of conformers was obtained

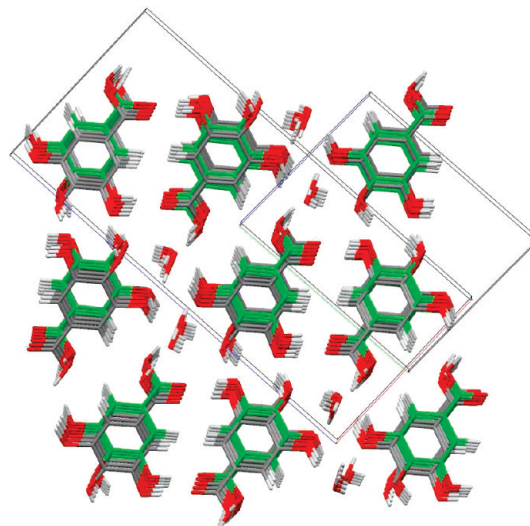
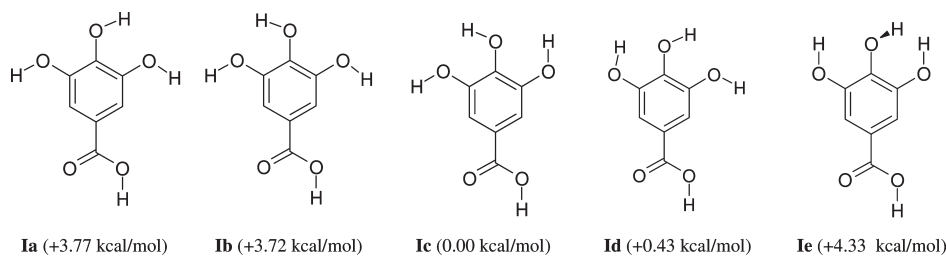


Figure 11. Packing overlay of predicted and experimental crystal structure of gallic acid monohydrate.

Scheme 5



from the analysis of known hydrate structures of 1,2,3-trihydroxybenzene derivatives (Supporting Information).

Prediction Results. Our prediction results show that the closest match ($P\bar{1}$; 3.533, 11.174, 9.309 Å; 84.85, 104.47, 98.82°) to the experimental structure ($P2_1/c$; 9.790, 3.609, 21.583 Å; 90, 91.46, 90°) has an overall rank of 141 (taking into account predicted structures from all the conformations and with different water positions) and an individual rank of 32 of conformer Ib hydrates. A structural overlay of the predicted and the experimental structure XXI is shown in Figure 11.

■ ASSOCIATED CONTENT

§ Supporting Information. Experimental, computational details, and crystallographic information files (CIF). CCDC deposition numbers for the reported crystal structures (1–16): 818142–818165. This material is available free of charge via the Internet at <http://pubs.acs.org>.

■ AUTHOR INFORMATION

Corresponding Author

*Fax: (+91) 80-23602306; tel: (+91) 80-22933311; e-mail: desiraju@sscu.iisc.ernet.in.

■ ACKNOWLEDGMENT

A.M. thanks CSIR, India, for a Junior Research Fellowship. P.G. and T.S.T. thank the Indian Institute of Science for postdoctoral fellowships. G.R.D. thanks the DST for the award of a J. C. Bose fellowship. We thank the Rigaku Corporation, Tokyo, for their support through a generous loan of a RigakuMercury-375R/M CCD (XtaLAB mini) table-top diffractometer. P.G. is on leave from the Department of Pharmaceutical Technology, Poznan University of Medical Sciences, Grunwaldzka 6, 60-780 Poznan, Poland; Fax: +48 61 8546666; Tel: +48 61 8546655.

■ REFERENCES

- (1) Blagden, N.; Davey, R. J. *J. Cryst. Growth Des.* **2003**, *3*, 873–885.
- (2) McCrone, W. C. *Physics and Chemistry of the Organic Solid State*; Fox, D.; Labes, M. M.; Weissberger, A., Eds.; Interscience Publishers: London, 1965; Vol. 2, pp 725–767.
- (3) (a) Kojima, T.; Tsutsumi, S.; Yamamoto, K.; Ikeda, Y.; Moriaki, T. *Int. J. Pharm.* **2010**, *399*, 52–59. (b) Morissette, S. L.; Almarsson, Ö.; Peterson, M. L.; Remenar, J. F.; Read, M. J.; Lemmo, A. V.; Ellis, S.; Cima, M. J.; Gardner, C. R. *Adv. Drug Delivery Rev.* **2004**, *56*, 275–300.
- (4) (a) Ouvrard, C.; Price, S. L. *J. Cryst. Growth Des.* **2004**, *4*, 1119–1127. (b) Vishweshwar, P.; McMahon, J.; Oliveira, M.; Peterson, M.; Peterson, M. L.; Zaworotko, M. J. *J. Am. Chem. Soc.* **2005**, *127*, 16802–16803. (c) Bond, A. D.; Boese, R.; Desiraju, G. R. *Angew. Chem., Int. Ed.* **2007**, *46*, 615–617. (d) Bond, A. D.; Boese, R.; Desiraju, G. R. *Angew. Chem., Int. Ed.* **2007**, *46*, 618–622. (e) Bond, A. D.; Solanko, K. A.; Parsons, S.; Redder, S.; Boese, R. *CrystEngComm* **2011**, *13*, 399–401.
- (5) (a) Vishweshwar, P.; Nangia, A.; Lynch, V. M. *CrystEngComm* **2003**, *5*, 164–168. (b) Lavender, E. S.; Glidewell, C.; Ferguson, G. *Acta Crystallogr. Sect. C* **1998**, *54*, 1637–1639. (c) Coupar, P. I.; Glidewell, C.; Ferguson, G. *Acta Crystallogr. Sect. B* **1997**, *53*, 521–533. (d) Desiraju, G. R. *Angew. Chem., Int. Ed. Engl.* **1995**, *34*, 2311–2327. (e) Subramanian, S.; Zaworotko, M. J. *Coord. Chem. Rev.* **1994**, *137*, 357–401. (f) Fan, E.; Vincent, C.; Geib, S. J.; Hamilton, A. D. *Chem. Mater.* **1994**, *6*, 1113–1117. (g) Desiraju, G. R. *Crystal Engineering: The Design of Organic Solids*; Elsevier: Amsterdam, 1989.
- (6) (a) MacGillivray, L. R. *CrystEngComm* **2002**, *4*, 37–41. (b) MacGillivray, L. R.; Reid, J. L.; Ripmeester, J. A. *J. Am. Chem. Soc.* **2000**, *122*, 7817–7818. (c) Anderson, S.; Anderson, H. L. In *Templated Organic Synthesis*; Diederich, F., Stang, P. J., Eds.: Wiley-VCH: New York, 2000. (d) MacGillivray, L. R.; Atwood, J. L. *J. Am. Chem. Soc.* **1997**, *119*, 6931–6932. (e) Feldman, K. S.; Campbell, R. F. *J. Org. Chem.* **1995**, *60*, 1924–1925.
- (7) (a) *CrystalClear 2.0*; Rigaku Corporation: Tokyo, Japan. (b) Pflugrath, J. W. *Acta Crystallogr. Sect. D* **1999**, *55*, 1718–1725.
- (8) Sheldrick, G. M. *SHELX97, Program for Crystal Structure Refinement*; University of Göttingen: Germany, 1997.
- (9) Farrugia, L. J. *J. Appl. Crystallogr.* **1999**, *32*, 837–838.
- (10) (a) Becke, A. D. *J. Chem. Phys.* **1993**, *98*, 5648–5652. (b) Lee, C.; Yang, W.; Parr, R. G. *Phys. Rev. B* **1988**, *37*, 785–789.
- (11) Gaussian 09, Revision A.02; Frisch, M. J.; Trucks, G. W.; Schlegel, H. B.; Scuseria, G. E.; Robb, M. A.; Cheeseman, J. R.; Scalmani, G.; Barone, V.; Mennucci, B.; Petersson, G. A.; Nakatsuji, H.; Caricato, M.; Li, X.; Hratchian, H. P.; Izmaylov, A. F.; Bloino, J.; Zheng, G.; Sonnenberg, J. L.; Hada, M.; Ehara, M.; Toyota, K.; Fukuda, R.; Hasegawa, J.; Ishida, M.; Nakajima, T.; Honda, Y.; Kitao, O.; Nakai, H.; Vreven, T.; Montgomery, J. A., Jr.; Peralta, J. E.; Ogliaro, F.; Bearpark, M.; Heyd, J. J.; Brothers, E.; Kudin, K. N.; Staroverov, V. N.; Kobayashi, R.; Normand, J.; Raghavachari, K.; Rendell, A.; Burant, J. C.; Iyengar, S. S.; Tomasi, J.; Cossi, M.; Rega, N.; Millam, N. J.; Klene, M.; Knox, J. E.; Cross, J. B.; Bakken, V.; Adamo, C.; Jaramillo, J.; Gomperts, R.; Stratmann, R. E.; Yazyev, O.; Austin, A. J.; Cammi, R.; Pomelli, C.; Ochterski, J. W.; Martin, R. L.; Morokuma, K.; Zakrzewski, V. G.; Voth, G. A.; Salvador, P.; Dannenberg, J. J.; Dapprich, S.; Daniels, A. D.; Farkas, Ö.; Foresman, J. B.; Ortiz, J. V.; Cioslowski, J.; Fox, D. J. Gaussian, Inc.: Wallingford, CT, 2009.
- (12) Farkas, O.; Schlegel, H. B. *Phys. Chem. Chem. Phys.* **2002**, *4*, 11–15.
- (13) Jetti, R. K. R.; Boese, R.; Sarma, J. A. R. P.; Reddy, L. S.; Vishweshwar, P.; Desiraju, G. R. *Angew. Chem., Int. Ed.* **2003**, *42*, 1963–1967.
- (14) Kitaigorodskii, A. I. *Organic Chemical Crystallography*; Consultants Bureau: New York, 1961 (originally published in Russian by the Press of the Academy of Sciences of the USSR, Moscow, 1955); Spek, A. L. Single-crystal structure validation with the program PLATON. *J. Appl. Crystallogr.* **2003**, *36*, 7–13.
- (15) Allen, F. H. *Acta Crystallogr., Sect. B* **2002**, *58*, 380–388.
- (16) Pickering, M.; Small, R. W. H. *Acta Crystallogr. Sect. B* **1982**, *38*, 3161–3163.
- (17) Bis, J. A.; Vishweshwar, P.; Weyna, D.; Zaworotko, M. J. *Mol. Pharmaceutics* **2007**, *4*, 401–416.
- (18) Mukherjee, A.; Desiraju, G. R. *Chem. Commun.* **2011**, *47*, 4090–4092.
- (19) Karki, S.; Frisčić, T.; Fábián, L.; Jones, W. *CrystEngComm* **2010**, *12*, 4038–4041.
- (20) (a) Varughese, S.; Desiraju, G. R. *Cryst. Growth Des.* **2010**, *10*, 4184–4196. (b) Clarke, H. D.; Arora, K. K.; Bass, H.; Kavuru, P.; Ong, T. T.; Pujari, T.; Wojtas, Ł.; Zaworotko, M. J. *Cryst. Growth Des.* **2010**, *10*, 2152–2167.
- (21) (a) van Eijck, B. P.; Kroon, J. *Acta Crystallogr., Sect. B* **2000**, *56*, 535–542. (b) Hulme, A. T.; Price, S. L. *J. Chem. Theory Comput.* **2007**, *3*, 1597–1608.
- (22) Clarke, H. D.; Arora, K. K.; Wojtas, Ł.; Zaworotko, M. J. *Cryst. Growth Des.* **2011**, *11*, 964–966.
- (23) Bardwell, D. A.; Adjiman, C. S.; Ammon, H. L.; Arnautova, E. A.; Bartashevich, E.; Boerriger, S. X. M.; Braun, D. E.; Cruz-Cabeza, A. J.; Day, G. M.; Della Valle, R. G.; Desiraju, G. R.; van Eijck, B. P.; Facelli, J. C.; Ferrao, M. D.; Grillo, D.; Habgood, M.; Hofmann, D. W. M.; Hofmann, F.; Jose, J.; Karamertzanis, P. G.; Kazantsev, A. V.; Kendrick, J.; Kuleshova, L. N.; Leusen, F. J. J.; Maleev, A.; Misquitta, A. J.; Mohamed, S.; Needs, R. J.; Neumann, M. A.; Nikylov, D.; Orendt, A. M.; Pal, R.; Pantelides, C. C.; Pickard, C. J.; Price, L. S.; Price, S. L.; Scheraga, H. A.; van de Streek, J.; Thakur, T. S.; Tiwari, S.; Venuti, E.; Zhitkov, I. *Acta Crystallogr., Sect. B*, in preparation.